Fibronectin matrix assembly is essential for cell condensation during chondrogenesis

Purva Singh and Jean E. Schwarzbauer

Department of Molecular Biology

Princeton University

Princeton, NJ 08544-1014 USA

Running head: Fibronectin matrix and condensation

Key words: Fibronectin matrix assembly, condensation, chondrogenesis, diastrophic dysplasia sulfate transporter

Address correspondence to:

Jean Schwarzbauer, Ph.D.

Department of Molecular Biology

Princeton University

Princeton, NJ 08544-1014 USA

Phone: (609) 258-2893

FAX: (609) 258-1035

jschwarz@princeton.edu

JCS Advance Online Article. Posted on 21 August 2014

Summary

Mesenchymal cell condensation is the initiating event in endochondral bone formation. Cell condensation is followed by differentiation into chondrocytes accompanied by induction of chondrogenic gene expression. Gene mutations involved in chondrogenesis cause chondrodysplasias and other skeletal defects. Using mesenchymal stem cells (MSCs) in an *in vitro* chondrogenesis assay, we found that knockdown of the diastrophic dysplasia sulfate transporter (DTDST), which is required for normal cartilage development, blocked cell condensation and caused a significant reduction in fibronectin matrix. Knockdown of fibronectin with siRNAs also blocked condensation. Fibrillar fibronectin matrix is detected prior to cell condensation and levels increased during and after condensation. Inhibition of fibronectin matrix assembly by the functional upstream domain (FUD) prevented cell condensation by MSCs and also by the chondrogenic cell line ATDC5. Our data show that cell condensation and induction of chondrogenesis depend on fibronectin matrix assembly and DTDST and indicate that this transporter is required earlier in chondrogenesis than previously appreciated. They also raise the possibility that certain of the skeletal defects in DTD patients might derive from the link between DTDST, fibronectin matrix, and condensation.

Introduction

Cartilage development is initiated by aggregation of undifferentiated mesenchyme into a condensed mass of cells. These condensed cells undergo differentiation to form chondrocytes that deposit cartilage-specific extracellular matrix (ECM). Differentiated chondrocytes can follow two fates: one is to continue to proliferate and maintain a cartilaginous structure and function, the second is to undergo hypertrophy. Hypertrophic chondrocytes undergo apoptosis leaving behind a mineralized matrix that acts as a template for osteoblasts (Lefebvre and Bhattaram, 2010; Singh and Schwarzbauer, 2012; Sundelacruz and Kaplan, 2009). One of the key features of chondrogenesis is a temporal change in the composition of the ECM (Singh and Schwarzbauer, 2012). During condensation, matrix proteins like fibronectin, collagen I, and the proteoglycan versican are prevalent (Dessau et al., 1980; Kamiya et al., 2006; Kimata et al., 1986; Kulyk et al.,

1991). In contrast, matrix deposited by differentiated chondrocytes is rich in collagens II and IX and the proteoglycan aggrecan (Choocheep et al., 2010; Knudson and Knudson, 2001; Knudson and Toole, 1985; Kravis and Upholt, 1985; Kulyk et al., 1991); this matrix may provide the optimal stiffness which is known to be important for chondrocyte differentiation (Allen et al., 2012).

Mesenchymal condensation is a prerequisite for chondrogenesis and is facilitated by cell adhesion molecules (Barna and Niswander, 2007; Bobick et al., 2009; DeLise et al., 2000). Up-regulation of the cell-cell adhesion proteins N-cadherin and neural cell adhesion molecule (N-CAM) is a hallmark of condensing cells (Bobick et al., 2009; Singh and Schwarzbauer, 2012) and condensation is reduced with loss of N-cadherin function (Bobick et al., 2009; DeLise and Tuan, 2002a; DeLise and Tuan, 2002b). Among the matrix proteins, fibronectin is abundant in mesenchyme and is up-regulated during condensation *in vivo* and *in vitro* (Dessau et al., 1980; Kulyk et al., 1989). Interactions involving the amino-terminal domain of fibronectin and heparinase-sensitive molecules on mesenchymal cell surfaces have been implicated in condensation (Frenz et al., 1989). Fibronectin is a ubiquitous ECM protein that is assembled into a fibrillar matrix through a cell-mediated process and links cells with collagens and other ECM proteins (Kadler et al., 2008; Singh and Schwarzbauer, 2012). However, an essential role for fibronectin matrix assembly during precartilage condensation has not been demonstrated.

Diastrophic dysplasia sulfate transporter (DTDST) has an essential role in the sulfation of glycosaminoglycans (GAGs) on cartilage proteoglycans and mutations in human DTDST result in skeletal defects including achondrogenesis and chondrodysplasias (Rossi and Superti-Furga, 2001). A DTDST knock-in mutant mouse model that disrupts DTDST function leads to defects in chondrocyte size, proliferation and terminal differentiation (Forlino et al., 2005; Gualeni et al., 2010). DTDST is also required for fibronectin matrix assembly by HT1080 fibrosarcoma cells (Galante and Schwarzbauer, 2007) suggesting that it might play a role prior to chondrocyte differentiation at a time when fibronectin matrix is being assembled.

A micromass culture technique is commonly used to study the mechanisms of chondrogenesis *in vitro* because it recapitulates the cell condensation and early

differentiation stages. We utilized bone marrow-derived mesenchymal stem cells (MSCs) and the chondrogenic cell line ATDC5 to assess the role of fibronectin during condensation. We show that fibronectin matrix is present before, during and after condensation. Its assembly into a matrix is dependent on DTDST and it plays an essential role in the condensation process.

Results

Timing of cell condensation after induction of chondrogenesis

MSCs were induced to initiate chondrogenic differentiation using high-density micromass cultures in chondrogenic medium containing TGFβ3. Cell rearrangements were visualized by time-lapse video microscopy (Fig 1A; Supplemental movie 1). The process of condensation begins as early as 2 hrs after induction when cells interact with neighboring cells and form small, interconnected cell clusters (Fig 1A, 3h 40m), which subsequently coalesce (Fig 1A, 7h 20m) and condense within 11 hrs to form a single opaque cohesive mass of cells (Fig 1A, 10h 40m). The cell condensate usually detaches from the substrate into the chondrogenic medium. For video microscopy, micromass cultures were plated on a glass-bottom culture dish. When plated on tissue culture plastic, the process is slightly slower. Across 17 micromass cultures on tissue culture plastic dishes, condensation was complete between 14 and 16 hrs. The progression of condensation was confirmed by increased staining at 24 hr with fluorescent peanut agglutinin, which detects precartilage cell aggregates and is a marker of condensation (Aulthouse and Solursh, 1987) (Fig 1B). Uninduced MSCs grown in monolayer showed negligible staining with peanut agglutinin (data not shown). N-cadherin is required for condensation to occur, but is subsequently down-regulated during differentiation (Bobick et al., 2009; Oberlender and Tuan, 1994; Woods et al., 2007). Our results show completion of condensation within 24 hr and since differentiation follows over a period of days, cell lysates were prepared over an 8-day time course. We found that N-cadherin protein was increased during the first 24 hrs and then declined gradually over the next 7 days (Fig 1C).

To show the initiation of the chondrogenic differentiation program, quantitative

RT-PCR (qPCR) was used to follow changes in gene expression during and after condensation of sex determining region (SRY) box 9 (Sox9), an essential transcription factor for chondrogenic differentiation (Bi et al., 1999; Healy et al., 1999). Sox9 was up-regulated more than 6-fold within 8 hrs and further increased to 9-fold by 16 hrs when condensation was complete. Post-condensation expression levels of Sox9 were down-regulated to about 2.5-fold by 48 hrs and then were maintained at that level for at least 6 days after induction (Fig 2A). Accumulation of GAGs in the ECM is a marker for chondrogenesis (Knudson and Knudson, 2001). GAGs detected with Alcian blue dye increased between 18 and 48 hrs (Fig 2B). Together, the cell rearrangements observed by time-lapse microscopy, the expression changes for N-cadherin and Sox9, and increased GAG deposition and lectin binding match the reported changes during condensation and chondrogenesis *in vivo* and *in vitro* (Barna and Niswander, 2007; Bobick et al., 2009; Brady et al., 2013; Chen et al., 2009; DeLise and Tuan, 2002b; Oberlender and Tuan, 1994). Taken together, the results in Figures 1 and 2 show that MSCs in micromass culture condense within the first 24 hr and then undergo chondrogenic differentiation over the following days.

DTDST is required for MSC condensation

DTDST plays an important role in cartilage development and homeostasis (Forlino et al., 2005; Rossi and Superti-Furga, 2001). To test whether this transporter is required for condensation, expression was knocked down in MSCs using DTDST siRNAs (Galante and Schwarzbauer, 2007). Quantitative RT-PCR (qPCR) showed more than 70% reduction in DTDST mRNA with this treatment (Fig 3A). Condensation of siRNA-treated cells was significantly impaired compared to mock-treated control cells (Fig 3B). Four out of 4 mock-treated cultures condensed whereas none of the DTDST knockdown cultures (0/4) condensed by 3 days. Therefore, in addition to its established role in the later stages of cartilage development, DTDST is required for the early, condensation stage of chondrogenesis. We have previously shown that fibronectin matrix assembly depends on the fibronectin-binding proteoglycan syndecan-2 and proteoglycan sulfation downstream of DTDST (Galante and Schwarzbauer, 2007). Therefore, we tested whether

condensation defects observed with DTDST knockdown were correlated with defects in fibronectin matrix assembly. Day 3 micromass cultures were solubilized in DOC buffer; mock-treated micromass cultures were condensed by that time but DTDST knockdown cultures were not. During matrix assembly, fibronectin is initially assembled into deoxycholate (DOC) detergent-soluble fibrils. DOC-soluble fibronectin levels in these lysates were significantly decreased with DTDST siRNA treatment (Fig 3C). Quantification of band intensities showed that DOC-soluble fibronectin was reduced 3-fold compared to the control (Fig 3D). DTDST knockdown does not change fibronectin expression levels (data not shown). Thus, there is a strong correlation between loss of condensation and reduction in fibronectin matrix assembly with knockdown of DTDST.

Fibronectin matrix assembly during condensation

The noticeable reduction in fibronectin matrix in DTDST knockdown cells (Fig 3C and D) and the reported increase in fibronectin mRNA levels during condensation in chick limb buds (Kulyk et al., 1989) led us to examine fibronectin during condensation and differentiation by MSCs in micromass cultures. qPCR was performed with RNA isolated over the time course of condensation and differentiation. Fibronectin is expressed by undifferentiated MSCs (data not shown) and its expression is maintained throughout condensation. Levels increased post-condensation as detected at 24 and 48 hrs (Fig 4A). In order to determine the fate of fibronectin, we investigated fibronectin matrix assembly by immunofluorescence staining of micromass cultures or of sections of differentiating cell aggregates. Fibronectin matrix fibrils are evident prior to condensation and as early as 6 hrs in micromass culture (Fig 4B). Fibronectin matrix continues to accumulate throughout condensation and differentiation as shown by staining of day 3 and day 6 cell aggregates (Fig 4C). Therefore, MSCs express and assemble fibronectin into a matrix throughout condensation and differentiation. Comparison to Figs 1B and 2 shows that fibronectin assembly occurs concomitant with changes in condensation and chondrogenic markers. The assembly of fibrillar fibronectin matrix prior to and during the time that cells are condensing suggests that fibronectin matrix may play a role in the condensation process.

Condensation is blocked by fibronectin knockdown

To determine whether fibronectin matrix is required for condensation, we used fibronectin siRNA transfection to knockdown expression in MSCs. This treatment had no obvious morphological effect on MSCs grown under non-differentiating conditions (data not shown). Fibronectin siRNA-treated MSCs induced to undergo chondrogenesis showed a significant reduction in fibronectin in the cell conditioned medium and in whole cell lysates compared to mock treated cells (Fig 5A). Therefore, siRNA treatment efficiently knocks down fibronectin expression and reduces or eliminates fibronectin matrix. Fibronectin siRNA-treated cells in a micromass culture showed delayed condensation (Fig 5B). After 3 days of induction, when all mock-treated micromass cultures were condensed (Fig 5B, CTL), only 5 out of 11 cultures with fibronectin siRNA-treated cells had condensed (Fig 5B, FN KD). The number of condensed cultures increased to 9 out of 11 by day 4. In the presence of exogenous fibronectin added to the fibronectin siRNA-treated cells, the majority of cultures had condensed by day 3 (12 out of 15; Fig 5B, FN KD+FN); the number of condensed cultures increased to 14 out of 15 by day 4 in conditions where exogenous fibronectin was added. These results show that fibronectin expression promotes cell condensation and that condensation can be rescued in fibronectin knockdown cultures by addition of fibronectin. It seems likely that condensation is delayed instead of completely blocked by fibronectin siRNAs because fibronectin expression is gradually restored in these cultures.

Condensation depends on fibronectin matrix assembly

To distinguish between a requirement for fibronectin expression and fibronectin matrix assembly during cell condensation, we used a 49 amino acid peptide from the functional upstream domain (FUD) of adhesin F1 of *Streptococcus pyogenes* to disrupt the assembly process. FUD binds to fibronectin's N-terminal assembly domain and prevents the fibronectin-fibronectin interactions that are essential for matrix assembly (Tomasini-Johansson et al., 2001). FUD does not affect FN expression ((Chiang et al., 2009) and

data not shown). The III-11C peptide derived from the III-11 module of fibronectin was used as a control (Bourdoulous et al., 1998; Chiang et al., 2009). Treatment of MSCs with FUD for 24 hrs in monolayer culture blocked matrix assembly (Fig 6A). Similarly, FUD reduced the incorporation of fibronectin into matrix fibrils in micromass cultures at 8 hrs, just prior to condensation (Fig 6B). Fibronectin matrix levels in an SDS lysate of a FUD-treated micromass culture were also reduced compared to III-11C treatment (Fig 6C) with six-fold lower fibronectin in lysates of FUD-treated micromass cultures compared to III-11C-treated cultures (Fig 6D). Seven FUD-treated micromass cultures failed to condense within three days whereas seven out of seven III-11C treated cultures were condensed by 24 hrs (Fig 7A). Time-lapse video microscopy of the condensation process in the presence of FUD shows that cells formed clusters but clusters failed to merge to form one condensed cell mass (Fig 7B, supplemental movie 3) while those with III-11C formed clusters that merged to form one cell condensate (Fig 7B, supplemental movie 2). These results show that inhibition of fibronectin matrix assembly is sufficient to inhibit condensation.

The generalizability of a role for fibronectin matrix in condensation was tested using ATDC5 cells, which condense into nodules when stimulated with insulin, transferrin and selenium (Fig 8A). Cultures with and without FUD were followed for 21 days. Nodule formation became apparent after 12 days of induction and the number and size of nodules continued to increase up to day 21 when total number of nodules was scored. Thirty-five nodules were detected with III-11C-treated ATDC5 cells, but only 6 nodules were observed in the FUD-treated cultures (Fig 8B). Fibronectin matrix levels were also reduced in the FUD-treated ATDC5 cultures (Fig 8C). Thus, the requirement for fibronectin matrix in condensation is not cell type-specific, since both MSCs and ATDC5 cells did not condense when fibronectin matrix assembly was prevented.

Discussion

Mesenchymal condensation is a prerequisite for chondrogenesis and is facilitated by cell adhesion molecules. Here we show an essential role for fibronectin matrix assembly, which is dependent on the sulfate transporter DTDST. Fibronectin is expressed and fibronectin matrix is assembled prior to and during condensation, and fibronectin matrix continues to accumulate during the post-condensation differentiation process. Knockdown of DTDST prevented condensation of micromass cultures concomitantly with reducing fibronectin matrix levels. Direct blockade of fibronectin matrix assembly completely inhibited condensation. Similar results were obtained using two distinctly different cell lines, mesenchymal stem cells and the ATDC5 chondrogenic cell line. Our results show that fibronectin fibril assembly is an important factor in bringing cells together at the earliest stage of mesenchymal cell differentiation into chondrocytes.

Fibronectin mRNA and protein levels are up-regulated at the time of condensation in chick limb bud mesenchyme (Dessau et al., 1980; Kulyk et al., 1989). Fibronectin is present in areas of chick limbs where condensed cells are differentiating as well as in growth plate cartilage in chick and mouse (Bobick et al., 2009; Gehris et al., 1997; Imai et al., 2007; Melnick et al., 1981; Singh and Schwarzbauer, 2012) (unpublished results). Fibronectin splice variants also change during condensation and differentiation although what specific functions these variants perform has not been fully elucidated (White et al., 2003). Our results show that a critical function for fibronectin in condensation is matrix assembly. The amino-terminal domain of fibronectin has previously been implicated in condensation, and the activity of this domain was attributed to interactions with cell surface heparin-like moieties but not to its role in matrix assembly (Frenz et al., 1989). FUD binds to the amino-terminal domain of fibronectin but does not compete with heparin for binding (Ensenberger et al., 2001). Therefore, our results showing the inhibition of condensation by FUD clearly connect matrix assembly with condensation independent of heparin binding to the amino-terminal domain.

In addition to its early role in promoting condensation, fibronectin matrix is continuously present post-condensation and in cartilage suggesting that fibronectin has temporally distinct roles in this tissue. Since fibronectin matrix acts as a platform for type I collagen

deposition (Kadler et al., 2008; Singh et al., 2010), one possibility is that fibronectin matrix has a similar role in type II collagen assembly during chondrocyte differentiation. Fibronectin matrix may also contribute to the chondrogenic differentiation program through effects on Sox9 expression. We observed a 25% reduction in Sox9 mRNA levels with 24 hr of FUD treatment compared to III-11C-treated cells (P.S., unpublished observations) indicating that matrix assembly may enhance Sox9 expression. We showed previously that mammary epithelial to mesenchymal transition depends on synergy between fibronectin and TGFβ signals (Park and Schwarzbauer, 2014). It is also possible that differentiation or maintenance of chondrocytes depends on synergistic signaling between fibronectin matrix and chondrogenic factors such as BMPs or TGFβ.

The process of condensation is governed by cell-cell interactions. N-cadherin is transiently up-regulated during cell condensation and declines thereafter (DeLise and Tuan, 2002b). NCAM is also enriched in cells undergoing condensation (Widelitz et al., 1993). Condensation and subsequent differentiation in micromass cultures are perturbed by cell manipulations that block NCAM or N-cadherin homotypic interactions or thatprevent connections via the cytoplasmic domain of N-cadherin (Bobick et al., 2009; DeLise and Tuan, 2002a; DeLise and Tuan, 2002b; Widelitz et al., 1993). In the absence of N-cadherin, such as in N-cadherin-null limb bud explants, condensation is not affected and proceeds through compensation by cadherin-11 (Luo et al., 2005). As in other studies, our results also show transient up-regulation of N-cadherin that coincides with the condensation timeline and with the early stages of fibronectin matrix assembly. Both cadherins and fibronectin matrix have been shown to be important for cell-cell cohesion (Robinson et al., 2004; Robinson et al., 2003) and fibronectin matrix assembly has been shown to decrease N-cadherin adhesion in fibroblasts (Lefort et al., 2011). The temporal connection between N-cadherin and fibronectin matrix suggests cooperation during condensation between these two adhesion systems. Any cooperation does not appear to be at the level of expression since N-cadherin protein levels were the same in FUD-treated and III-11C-treated micromass cultures undergoing condensation (P.S., unpublished observations).

Fibronectin matrix assembly is also linked to chondrogenesis through the role of DTDST in this process. Mutations in this transporter cause a variety of chondrodysplasias of varying severity including diastrophic dysplasia, multiple epiphyseal dysplasia, atelosteogenesis type 2 and achondrogenesis 1B (Karniski, 2001; Superti-Furga et al., 1996a; Superti-Furga et al., 1996b). Sulfated proteoglycans are abundant in cartilage matrix (Knudson and Knudson, 2001) and a main molecular defect in DTD patients is undersulfation of cartilage proteoglycans. We found that sulfate deficiency dramatically reduces fibronectin matrix assembly by fibrosarcoma cells and linked this matrix defect to DTDST and syndecan-2, a fibronectin-binding, transmembrane proteoglycan (Galante and Schwarzbauer, 2007). Knockdown of DTDST in fibrosarcoma cells reduced fibronectin matrix, and expression of a DTDST transgene promoted fibronectin assembly, showing the importance of this transporter in facilitating the assembly process (Galante and Schwarzbauer, 2007). Here we showed that loss of DTDST reduces fibronectin matrix as it impairs mesenchymal cell condensation. This condensation defect occurs earlier in cartilage development than the previously characterized undersulfation defects suggesting that DTDST may have multiple roles during chondrogenesis. Not only have we identified early roles for DTDST and fibronectin matrix in chondrogenesis, but the link to fibronectin matrix raises the possibility that effects of mutations in DTDST that cause chondrodysplasias might be mediated in part by its effect on fibronectin matrix during cartilage development.

Materials and Methods

Cell culture - Bone marrow-derived mesenchymal stem cells obtained from Lonza (Walkersville, MD, USA) had been confirmed as positive for stem cell markers and negative for lineage-specific markers by flow cytometry and were certified for differentiation as described by Lonza. In addition to our chondrogenesis experiments, we also verified their ability to undergo differentiation along adipogenic and osteogenic lineages (data not shown). MSCs were maintained in an undifferentiated state by

culturing in defined mesenchymal stem cell basal medium (MSCBM) containing 10% serum plus growth supplements, L-glutamine and GA1000 (Lonza, Walkersville, MD, USA). Cells were passaged at 80-90 % confluence and replated at a density of 5000-6000 cells/cm^2. Cells were used for experiments up to passage 8. The ATDC5 cell line (Sigma, St Louis, MO, USA) was maintained in DMEM: F12 (1:1) (Life Technologies, Grand Island, NY, USA) supplemented with 5 % fetal bovine serum (Hyclone, Logan, UT, USA). All cultures were grown at 37 ˚C and 5 % CO_2

In vitro chondrogenesis assay - To establish high-density cultures for chondrogenesis, MSCs grown in monolayer were trypsinized, counted and then induced in either micromass culture or pellet culture. Chondrogenic differentiation medium is composed of chondrogenic basal medium supplemented with dexamethasone, ascorbate, ITS + supplement, GA1000, sodium pyruvate, proline, L-glutamine (Lonza, Walkersville, MD, USA); TGFβ3 was added at 10ng/ml concentration (Lonza, Walkersville, MD, USA). Differentiation medium is serum-free so all fibronectin present in the condensing cultures is produced by the MSCs. For pellet culture, 2 $x10^5$ cells in chondrogenic differentiation medium without TGFβ3 were centrifuged at 1000 rpm for 5 min, cells were resuspended in chondrogenic differentiation medium with TGFβ3 and then centrifuged again to form a cell pellet (as recommended in the Lonza protocol). For micromass cultures, 50,000, 70,000 or 100,000 cells in 10 µl of MSCBM were plated on tissue culture plastic for 45 min to allow adhesion and then chondrogenic differentiation medium containing TGFβ3 was added. For establishing the condensation time line, each independent experiment was performed using 4-5 micromass cultures.

ATDC5 cells were either plated at 4 x 10^4 cells/well of a 12-well plate or 6 x 10^4 cells / well of 6-well plate in maintenance medium and allowed to grow to confluence for 4 days prior to adding differentiation medium. Differentiation medium is maintenance medium supplemented with Insulin-Transferrin-Selenium (ITS) (Life Technologies, Grand Island, NY, USA). Nodules were counted at day 21.

In experiments with peptide addition, III-11C or FUD was added with differentiation medium. Both III-11C and FUD were used at 0.3 µM. His-tagged III-11C and FUD were purified as described (Hunt et al., 2012).

Quantitative RT-PCR - Cells were lysed in Trizol reagent (Life Technologies, Grand Island, NY, USA) and, after chloroform extraction and ethanol precipitation, RNA was subjected to RNeasy purification according to the manufacturer's instructions (Qiagen, Hilden, Germany). 500 ng of total RNA was reversed transcribed using random hexamer primers and Superscript II reverse transcriptase (Life Technologies, Grand Island, NY, USA). Primers for real-time PCR were designed using Mac Vector and reactions performed in a mix containing Brilliant(R) II SYBR QPCR Low Rox Master Mix (Agilent Technologies, Waldbronn, Germany) and 200 nM of each primer on the Mx3000P QPCR System (Agilent Technologies, Waldbronn, Germany). PCR reaction conditions were: 10 minutes at 95 ˚C, followed by 40 cycles of 30 seconds at 95 ˚C, 60 seconds at 60 ˚C, 60 seconds at 72 ˚C. Data analysis was performed using MxPro TM QPCR Software (Agilent Technologies, Waldbronn, Germany). All data values were normalized to Ubiquitin C (UBC). 5' to 3' sequences of forward and reverse primers used in this study are: Sox9 Forward/Reverse - ACC AGT ACC CGC ACT TGC AC / CTT CAC CGA CTT CCT CCG CCG; Ubiquitin C Forward/Reverse - ATT TGG GTC GCG GTT CTT / TGC CTT GAC ATT CTC GAT GGT; Fibronectin Forward/Reverse - AAA CTT GCA TCT GGA GGC AAA CCC / AGC TCT GAT CAG CAT GGA CCA CTT; DTDST Forward/Reverse - TTG TGT CAT CCT CCG CAC TCA GAA / TGA TGC CTG GCT TAG TCT GAA GGT.

Cell lysis and immunoblotting

Cells were lysed in modified RIPA buffer (Wierzbicka-Patynowski et al., 2007), urea-SDS buffer (8M urea, 2% SDS, 2% β-mercaptoethanol, 0.16 M Tris-HCl, pH 6.8), SDS buffer (2% SDS, 20mM Tris pH 8.8, 2mM EDTA, 2mM PMSF), or DOC buffer (2 % DOC, 20 mM Tris-HCl, pH 8.8, 2 mM EDTA, 2mM PMSF) supplemented with protease inhibitor cocktail (Roche Diagnostics, Indianapolis, IN, USA). DOC lysates were separated into DOC-soluble and DOC-insoluble material by centrifugation. DOC-soluble fibronectin was compared in Fig 3 because DTDST siRNA-treated cells do make detectable DOC-insoluble fibronectin matrix. For SDS lysis of ATDC5 cells, the SDS

concentration in SDS buffer was increased to 4%. Total protein concentration was determined using a BCA protein assay (Pierce Chemical Co., Rockford, IL, USA). Normalized, reduced samples were separated by SDS-PAGE, and proteins were detected by immunoblotting. Antibodies and dilutions were rabbit anti-GAPDH (1:2000, Cell Signaling, Danvers, MA, USA), mouse anti-fibronectin hybridoma supernatant (HFN7.1) (1:10000, (Galante and Schwarzbauer, 2007). R457 rabbit anti-fibronectin antiserum (1:2000, (Aguirre et al., 1994) anti-N-cadherin (mouse monoclonal 3B9, 1:500, Life Technologies, Grand Island, NY, USA), horseradish peroxidase-conjugated goat anti-rabbit IgG or goat anti-mouse IgG (Pierce Chemical Co., Rockford, IL, USA, 1:10000). Blots were developed using Super Signal West Pico Chemiluminescent substrate (Pierce Chemical Co., Rockford, IL, USA). Quantification of bands was done using Quantity One(R) software (Bio-Rad, Hercules, CA, USA).

siRNA transfection - Cells were plated in MSCBM at a density of 5000 cells/cm^2. After 24 hr, cells were transfected with 100 nM siRNAs for human fibronectin (siGENOME SMARTpool human FN1 siRNA, Thermo Scientific, Pittsburgh, PA, USA) or 120 nM siRNA for human DTDST in RNAiMax reagent (Life Technologies, Grand Island, NY, USA) (Galante and Schwarzbauer, 2007). Cells were incubated with siRNA and RNAimax cocktail diluted in 1 ml of Optimem for 4 hrs and then supplemented with 500 µl of complete medium. Controls included mock transfected cells treated with RNAiMax without siRNAs or cells transfected with control siRNAs (siControl Non-targeting siRNA#1, Thermo Scientific, Pittsburgh, PA, USA). On the following day, cells were replated in complete medium and allowed to recover for 3 days before starting the chondrogenesis assay. Condensation was somewhat slower in cells that had been exposed to siRNA transfection reagents. Both mock and control siRNA-treated cells condensed by day 3, at least 24 hr prior to condensation of the majority of fibronectin siRNA-treated cells, although mock-treated cells usually condensed 6-24 hrs earlier than control siRNA-treated cells. Levels of secreted fibronectin were not affected by either mock or control siRNA treatment. For fibronectin rescue experiments, exogenous rat plasma fibronectin was included at 10, 30 or 50 µg/ml in the high-density cultures as well as in the differentiation media.

Staining and microscopy - Pellet cultures from day 3 and 6 were embedded in optimal cutting temperature (OCT) medium (Electron Microscopy Sciences, Hatfield, PA, USA) and cryo-sectioned into 5 µm thick sections using a Leica CM 3050 S cryostat (Leica Biosystems, Buffalo Grove, IL, USA). Cells grown in monolayer for 24 hrs, micromass cultures grown on coverslips for 6 or 8 hrs or sections of condensed cultures were fixed in 3.7% (v/v) formaldehyde (Sigma, St. Louis, MO, USA) in PBS for 15 minutes at room temperature, washed with PBS, and blocked in 2 % BSA/PBS for an hour followed by incubation with HFN 7.1 (1:500) and Alexa 488 goat anti-mouse IgG (1:500, Invitrogen Life Technologies, Eugene, OR, USA) in 1% BSA/PBS. Coverslips were mounted on slides using Fluor guard Anti-Fade reagent (Bio-Rad, Hercules, CA, USA). Visualization was done using a Nikon TE2000U microscope (Chiyoda, Tokyo, Japan) equipped with a Cooke SensiCam QE High Performance camera using iVision software.

Condensed micromass cultures were washed in PBS and fixed in 95% methanol for 20 min followed by staining with 1 % Alcian blue stain in 0.1 N HCl overnight at 4^{o}C (Shukunami et al., 1996), washed with 0.1 N HCl, and rinsed with distilled water. Stained pellets were imaged by bright field microscopy using a Nikon Microphat SA microscope equipped with Nikon DS1500 color camera (Chiyoda, Tokyo, Japan).

For time-lapse video microscopy, micromass cultures on glass bottom dishes (Greiner Bio-one, Frickenhausen, Germany) were visualized for 16 hr from the time of induction using a Nikon A1RS microscope (Chiyoda, Tokyo, Japan) equipped with a motorized stage and a chamber with a forced-air heater, allowing for temperature and CO_2 control during time-lapse image acquisition. Bright field was utilized for image acquisition. Images were acquired every 10 min over a 16 hr time interval using an Andor SC Mos monochrome camera. Nis Elements 2 and Image J software were employed for time-lapse image analysis. Supplemental movies are a compilation of every sixth frame of 94 frames.

Staining with rhodamine-conjugated peanut agglutinin (Vector Laboratories, Burlingame, CA, USA) was performed on micromass cultures. Cells on coverslips were fixed in 4% paraformaldehyde in PBS for 30 min at 4 ˚C and stained with peanut agglutinin at 10 µg/ml in PBS for 2 hrs at room temperature. Coverslips were mounted and visualized as described above.

Statistical analysis – Graphs show average values of aggregated data. Error bars represent relative standard error (s.e.m.) or standard deviation in those cases in which the experiment was performed twice. For statistical analyses, two-tailed t-test or N1 chi-square test was used.

Acknowledgements

We would like to thank Dr. Gary Laevsky (Confocal Microscopy Core Facility) and Dr. Shelby Blythe (Princeton University) for help with time-lapse microscopy and movies, and Dr. Jane Sottile (University of Rochester) for FUD reagents. We would also like to thank Vivek Desai and Charles Miller for helpful scientific discussions. This research was funded by the National Institutes of Health (CA160611 to J.E.S).

References

Aguirre, K. M., McCormick, R. J. and Schwarzbauer, J. E. (1994). Fibronectin self-association is mediated by complementary sites within the amino-terminal one-third of the molecule. *J Biol Chem* **269**, 27863-8.

Allen, J. L., Cooke, M. E. and Alliston, T. (2012). ECM stiffness primes the TGFbeta pathway to promote chondrocyte differentiation. *Mol Biol Cell* **23**, 3731-42.

Aulthouse, A. L. and Solursh, M. (1987). The detection of a precartilage, blastema-specific marker. *Dev. Biol.* **120**, 377-384.

Barna, M. and Niswander, L. (2007). Visualization of cartilage formation: insight into cellular properties of skeletal progenitors and chondrodysplasia syndromes. *Dev. Cell* **12**, 931-941.

Bi, W., Deng, J. M., Zhang, Z., Behringer, R. R. and de Crombrugghe, B. (1999). Sox9 is required for cartilage formation. *Nat. Genet.* **22**, 85-89.

Bobick, B. E., Chen, F. H., Le, A. M. and Tuan, R. S. (2009). Regulation of the chondrogenic phenotype in culture. *Birth Defects Res. C Embryo Today* **87**, 351-371.

Bourdoulous, S., Orend, G., MacKenna, D. A., Pasqualini, R. and Ruoslahti, E. (1998). Fibronectin matrix regulates activation of RHO and CDC42 GTPases and cell cycle progression. *J Cell Biol* **143**, 267-76.

Brady, K., Dickinson, S. C., Guillot, P. V., Polak, J. M., Blom, A. W., Kafienah, W. and Hollander, A. P. (2013). Human fetal and adult bone marrow derived mesenchymal stem cells use different signalling pathways for the initiation of chondrogenesis. *Stem Cells Dev* **Epub ahead of publication**.

Chen, W. H., Lai, M. T., Wu, A. T., Wu, C. C., Gelovani, J. G., Lin, C. T., Hung, S. C., Chiu, W. T. and Deng, W. P. (2009). In vitro stage-specific chondrogenesis of mesenchymal stem cells committed to chondrocytes. *Arthritis Rheum.* **60**, 450-459.

Chiang, H. Y., Korshunov, V. A., Serour, A., Shi, F. and Sottile, J. (2009). Fibronectin is an important regulator of flow-induced vascular remodeling. *Arterioscler Thromb Vasc Biol* **29**, 1074-9.

Choocheep, K., Hatano, S., Takagi, H., Watanabe, H., Kimata, K. and Kongtawelert, P. (2010). Versican facilitates chondrocyte differentiation and regulates joint morphogenesis. *J. Biol. Chem.* **285**, 21114-21125.

DeLise, A. M., Fischer, L. and Tuan, R. S. (2000). Cellular interactions and signaling in cartilage development. *Osteoarthritis Cartilage* **8**, 309-34.

DeLise, A. M. and Tuan, R. S. (2002a). Alterations in the spatiotemporal expression pattern and function of N-cadherin inhibit cellular condensation and chondrogenesis of limb mesenchymal cells in vitro. *J Cell Biochem* **87**, 342-59.

DeLise, A. M. and Tuan, R. S. (2002b). Analysis of N-cadherin function in limb mesenchymal chondrogenesis in vitro. *Dev Dyn* **225**, 195-204.

Dessau, W., von der Mark, H., von der Mark, K. and Fischer, S. (1980). Changes in the patterns of collagens and fibronectin during limb-bud chondrogenesis. *J Embryol Exp Morphol* **57**, 51-60.

Ensenberger, M. G., Tomasini-Johansson, B. R., Sottile, J., Ozeri, V., Hanski, E. and Mosher, D. F. (2001). Specific interactions between F1 adhesin of Streptococcus pyogenes and N-terminal modules of fibronectin. *J Biol Chem* **276**, 35606-13.

Forlino, A., Piazza, R., Tiveron, C., Della Torre, S., Tatangelo, L., Bonafe, L., Gualeni, B., Romano, A., Pecora, F., Superti-Furga, A. et al. (2005). A diastrophic dysplasia sulfate transporter (SLC26A2) mutant mouse: morphological and biochemical characterization of the resulting chondrodysplasia phenotype. *Hum Mol Genet* **14**, 859-71.

Frenz, D. A., Jaikaria, N. S. and Newman, S. A. (1989). The mechanism of precartilage mesenchymal condensation: a major role for interaction of the cell surface with the amino-terminal heparin-binding domain of fibronectin. *Dev Biol* **136**, 97-103.

Galante, L. L. and Schwarzbauer, J. E. (2007). Requirements for sulfate transport and the diastrophic dysplasia sulfate transporter in fibronectin matrix assembly. *J Cell Biol* **179**, 999-1009.

Gehris, A. L., Stringa, E., Spina, J., Desmond, M. E., Tuan, R. S. and Bennett, V. D. (1997). The region encoded by the alternatively spliced exon IIIA in mesenchymal fibronectin appears essential for chondrogenesis at the level of cellular condensation. *Dev Biol* **190**, 191-205.

Gualeni, B., Facchini, M., De Leonardis, F., Tenni, R., Cetta, G., Viola, M., Passi, A., Superti-Furga, A., Forlino, A. and Rossi, A. (2010). Defective proteoglycan sulfation of the growth plate zones causes reduced chondrocyte proliferation via an altered Indian hedgehog signalling. *Matrix Biol.* **29**, 453-460.

Healy, C., Uwanogho, D. and Sharpe, P. T. (1999). Regulation and role of Sox9 in cartilage formation. *Dev Dyn* **215**, 69-78.

Hunt, G. C., Singh, P. and Schwarzbauer, J. E. (2012). Endogenous production of fibronectin is required for self-renewal of cultured mouse embryonic stem cells. *Exp Cell Res* **318**, 1820-31.

Imai, K., Dalal, S. S., Hambor, J., Mitchell, P., Okada, Y., Horton, W. C. and D'Armiento, J. (2007). Bone growth retardation in mouse embryos expressing human collagenase 1. *Am J Physiol Cell Physiol* **293**, C1209-15.

Kadler, K. E., Hill, A. and Canty-Laird, E. G. (2008). Collagen fibrillogenesis: fibronectin, integrins, and minor collagens as organizers and nucleators. *Curr. Opin. Cell Biol.* **20**, 495-501.

Kamiya, N., Watanabe, H., Habuchi, H., Takagi, H., Shinomura, T., Shimizu, K. and Kimata, K. (2006). Versican/PG-M regulates chondrogenesis as an extracellular matrix molecule crucial for mesenchymal condensation. *J Biol Chem* **281**, 2390-400.

Karniski, L. P. (2001). Mutations in the diastrophic dysplasia sulfate transporter (DTDST) gene: correlation between sulfate transport activity and chondrodysplasia phenotype. *Hum Mol Genet* **10**, 1485-90.

Kimata, K., Oike, Y., Tani, K., Shinomura, T., Yamagata, M., Uritani, M. and Suzuki, S. (1986). A large chondroitin sulfate proteoglycan (PG-M) synthesized before chondrogenesis in the limb bud of chick embryo. *J. Biol. Chem.* **261**, 13517-13525.

Knudson, C. B. and Knudson, W. (2001). Cartilage proteoglycans. *Semin Cell Dev Biol* **12**, 69-78.

Knudson, C. B. and Toole, B. P. (1985). Changes in the pericellular matrix during differentiation of limb bud mesoderm. *Dev Biol* **112**, 308-18.

Kravis, D. and Upholt, W. B. (1985). Quantitation of type II procollagen mRNA levels during chick limb cartilage differentiation. *Dev Biol* **108**, 164-72.

Kulyk, W. M., Coelho, C. N. and Kosher, R. A. (1991). Type IX collagen gene expression during limb cartilage differentiation. *Matrix* **11**, 282-288.

Kulyk, W. M., Upholt, W. B. and Kosher, R. A. (1989). Fibronectin gene expression during limb cartilage differentiation. *Development* **106**, 449-455.

Lefebvre, V. and Bhattaram, P. (2010). Vertebrate skeletogenesis. *Curr Top Dev Biol* **90**, 291-317.

Lefort, C. T., Wojciechowski, K. and Hocking, D. C. (2011). N-cadherin cell-cell adhesion complexes are regulated by fibronectin matrix assembly. *J Biol Chem* **286**, 3149-60.

Luo, Y., Kostetskii, I. and Radice, G. L. (2005). N-cadherin is not essential for limb mesenchymal chondrogenesis. *Dev Dyn* **232**, 336-44.

Melnick, M., Jaskoll, T., Brownell, A. G., MacDougall, M., Bessem, C. and Slavkin, H. C. (1981). Spatiotemporal patterns of fibronectin distribution during embryonic development. I. Chick limbs. *J Embryol Exp Morphol* **63**, 193-206.

Oberlender, S. A. and Tuan, R. S. (1994). Expression and functional involvement of N-cadherin in embryonic limb chondrogenesis. *Development* **120**, 177-87.

Park, J. and Schwarzbauer, J. E. (2014). Mammary epithelial cell interactions with fibronectin stimulate epithelial-mesenchymal transition. *Oncogene* **33**, 1649-57.

Robinson, E. E., Foty, R. A. and Corbett, S. A. (2004). Fibronectin matrix assembly regulates alpha5beta1-mediated cell cohesion. *Mol Biol Cell* **15**, 973-81.

Robinson, E. E., Zazzali, K. M., Corbett, S. A. and Foty, R. A. (2003). Alpha5beta1 integrin mediates strong tissue cohesion. *J Cell Sci* **116**, 377-86.

Rossi, A. and Superti-Furga, A. (2001). Mutations in the diastrophic dysplasia sulfate transporter (DTDST) gene (SLC26A2): 22 novel mutations, mutation review, associated skeletal phenotypes, and diagnostic relevance. *Hum Mutat* **17**, 159-71.

Shukunami, C., Shigeno, C., Atsumi, T., Ishizeki, K., Suzuki, F. and Hiraki, Y. (1996). Chondrogenic differentiation of clonal mouse embryonic cell line ATDC5 in vitro: differentiation-dependent gene expression of parathyroid hormone (PTH)/PTH-related peptide receptor. *J Cell Biol* **133**, 457-68.

Singh, P., Carraher, C. and Schwarzbauer, J. E. (2010). Assembly of fibronectin extracellular matrix. *Annu. Rev. Cell Dev. Biol.* **26**, 397-419.

Singh, P. and Schwarzbauer, J. E. (2012). Fibronectin and stem cell differentiation - lessons from chondrogenesis. *J Cell Sci* **125**, 3703-12.

Sundelacruz, S. and Kaplan, D. L. (2009). Stem cell- and scaffold-based tissue engineering approaches to osteochondral regenerative medicine. *Semin Cell Dev Biol* **20**, 646-55.

Superti-Furga, A., Hastbacka, J., Rossi, A., van der Harten, J. J., Wilcox, W. R., Cohn, D. H., Rimoin, D. L., Steinmann, B., Lander, E. S. and Gitzelmann, R. (1996a). A family of chondrodysplasias caused by mutations in the diastrophic dysplasia sulfate transporter gene and associated with impaired sulfation of proteoglycans. *Ann N Y Acad Sci* **785**, 195-201.

Superti-Furga, A., Hastbacka, J., Wilcox, W. R., Cohn, D. H., van der Harten, H. J., Rossi, A., Blau, N., Rimoin, D. L., Steinmann, B., Lander, E. S. et al. (1996b). Achondrogenesis type IB is caused by mutations in the diastrophic dysplasia sulphate transporter gene. *Nat Genet* **12**, 100-2.

Tomasini-Johansson, B. R., Kaufman, N. R., Ensenberger, M. G., Ozeri, V., Hanski, E. and Mosher, D. F. (2001). A 49-residue peptide from adhesin F1 of Streptococcus pyogenes inhibits fibronectin matrix assembly. *J Biol Chem* **276**, 23430-9.

White, D. G., Hershey, H. P., Moss, J. J., Daniels, H., Tuan, R. S. and Bennett, V. D. (2003). Functional analysis of fibronectin isoforms in chondrogenesis: Full-length recombinant mesenchymal fibronectin reduces spreading and promotes condensation and chondrogenesis of limb mesenchymal cells. *Differentiation* **71**, 251-61.

Widelitz, R. B., Jiang, T. X., Murray, B. A. and Chuong, C. M. (1993). Adhesion molecules in skeletogenesis: II. Neural cell adhesion molecules mediate precartilaginous mesenchymal condensations and enhance chondrogenesis. *J Cell Physiol* **156**, 399-411.

Wierzbicka-Patynowski, I., Mao, Y. and Schwarzbauer, J. E. (2007). Continuous requirement for pp60-Src and phospho-paxillin during fibronectin matrix assembly by transformed cells. *J Cell Physiol* **210**, 750-6.

Woods, A., Wang, G., Dupuis, H., Shao, Z. and Beier, F. (2007). Rac1 signaling stimulates N-cadherin expression, mesenchymal condensation, and chondrogenesis. *J Biol Chem* **282**, 23500-8.

Figure legends

Figure 1. MSCs undergo condensation in vitro. MSCs were induced to undergo condensation and then visualized by time-lapse video microscopy over 11 hrs. (A) Frames are from the indicated times: 0 hr, 3 hr 40 min, 7 hr 20 min and 10 hr 40 min. Results are representative of three experiments. Scale bar 1000 µm. [Also see Supplemental movie 1]. (B) Cells induced for 8 hr or 24 hr were stained with rhodamine-conjugated peanut agglutinin. Scale bar 50 µm. (C) Cell lysates were prepared with mRIPA buffer at the indicated times from MSCs undergoing chondrogenesis. Lysates were immunoblotted with anti-N-cadherin or anti-GAPDH antibodies.

Figure 2. Chondrogenic differentiation by MSCs. (A) RNA was isolated at the indicated times from MSCs induced to undergo chondrogenesis and used for quantitative RT-PCR with Sox9 and ubiquitin C primers. * $p < 0.05$ for four experiments at 0-48 hrs. The "6 day" column is the average of two experiments; the bar shows the range. (B) Condensed micromass cultures at 18 or 48 hrs were stained with Alcian blue. Scale bar 50 µm.

Figure 3: Loss of DTDST impairs condensation. MSCs treated with DTDST siRNAs or mock-treated were grown in monolayer for 2 days and then used for RNA isolation. Quantitative RT-PCR was performed with DTDST primers. *** $p < 0.0005$ for three experiments. (B) Bright field images are shown of mock-treated (CTL) or DTDST siRNA-treated (DTDST KD) micromass cultures on day 3. 4/4 and 0/4 indicate the number of condensed cultures out of total cultures for each treatment. Scale bar 100 µm. (C) DOC lysates were prepared on day 3 from mock or DTDST siRNA cultures and the DOC-soluble material was immunoblotted with anti-fibronectin (HFN7.1) or anti-GAPDH antibodies. (D) Graph shows quantification of bands in immunoblots from three experiments. ** $p < 0.005$.

Figure 4. Fibronectin matrix increases during condensation and differentiation. (A) Quantitative RT-PCR was performed on RNA isolated at indicated times after induction of chondrogenesis. * $p < 0.05$ from four independent experiments. (B) Micromass culture undergoing condensation for 6 hrs was stained with anti-fibronectin antibodies. Inset in left panel is shown at higher magnification on the right. Scale bar 50 µm. (C) Five µm sections of condensed cultures at 3 and 6 days were stained with anti-fibronectin antibodies. Scale bar 50 µm.

Figure 5: Loss of fibronectin delays condensation. MSCs were treated with FN siRNAs or mock-treated were induced to undergo condensation. At 2 days, conditioned media (CM) were collected and cultures were lysed in urea-SDS buffer. Fibronectin was isolated from media using gelatin beads. Medium fibronectin and cell lysates were separated by SDS-PAGE and analyzed by immunoblotting with anti-fibronectin and anti-GAPDH antibodies. (B) Cell aggregates resulting from condensation were imaged at day 3 or 4. By day 3, 16 out of 16 cultures were condensed with mock (CTL) treatment (B, top left). Only 5 of 11 FN knockdown (FN KD) cultures were condensed on day 3 (B, middle left) ($p < 0.0005$ compared to CTL). That number increased to 9 out of 11 by day 4 (B, middle right). The remaining two cultures condensed by day 5 and day 6. Twelve out of 15 FN KD cultures condensed by day 3 when supplemented with exogenous fibronectin (FN KD + FN) (B, bottom left) ($p < 0.03$ compared to FN KD); this number increased to 14 out 15 by day 4 (B, bottom right). The fifteenth culture condensed by day 5. Results are from seven independent condensation experiments. Scale bar 50 µm.

Figure 6. FUD inhibits fibronectin matrix assembly in micromass culture. MSCs grown in monolayer for 24 hrs in MSCBM (A) or in micromass culture in induction medium for 8 hrs (B) in presence of either 0.33 µM FUD or III-11C were stained with anti-fibronectin antibodies. Scale bar 50 µm. (C) At 8 hrs, cell lysates were prepared from micromass cultures in SDS buffer, lysates were separated by SDS-PAGE and analyzed

by immunoblotting with anti-fibronectin or anti-GAPDH antibodies. (D) Band intensities were quantified from two experiments. * $p < 0.05$.

Figure 7. Fibronectin matrix assembly is essential for condensation.

Pictures taken under bright field depict micromass cultures of MSCs induced to condense in the presence of 0.33 µM III-11C or FUD for 24 hrs (A). Seven cultures for each condition were analyzed. 7 out of 7 and 0 out of 7 condensed with III-11C and FUD, respectively. Scale bar 100 µm. (B) Time-lapse video microscopy of MSCs induced to undergo condensation. Frames are shown from the indicated times. Results are represented of movies from three independent cultures. Scale bar 1000 µm. [Also see Supplemental movie 2 and 3].

Figure 8: Fibronectin matrix assembly is required for nodule formation in ATDC5 cell cultures. (A) Bright field images depict areas of a differentiating ATDC5 culture with and without a nodule. Scale bar 50 µm. (B) Cumulative nodule numbers from three independent differentiating ATDC5 cultures grown in the presence of 0.33 µM FUD or III-11C at day 21. At 21 days, SDS cell lysates were prepared from differentiating ATDC5 cultures. Lysates were separated by SDS PAGE and analyzed by immunoblotting with anti-fibronectin or anti-GAPDH antibodies.

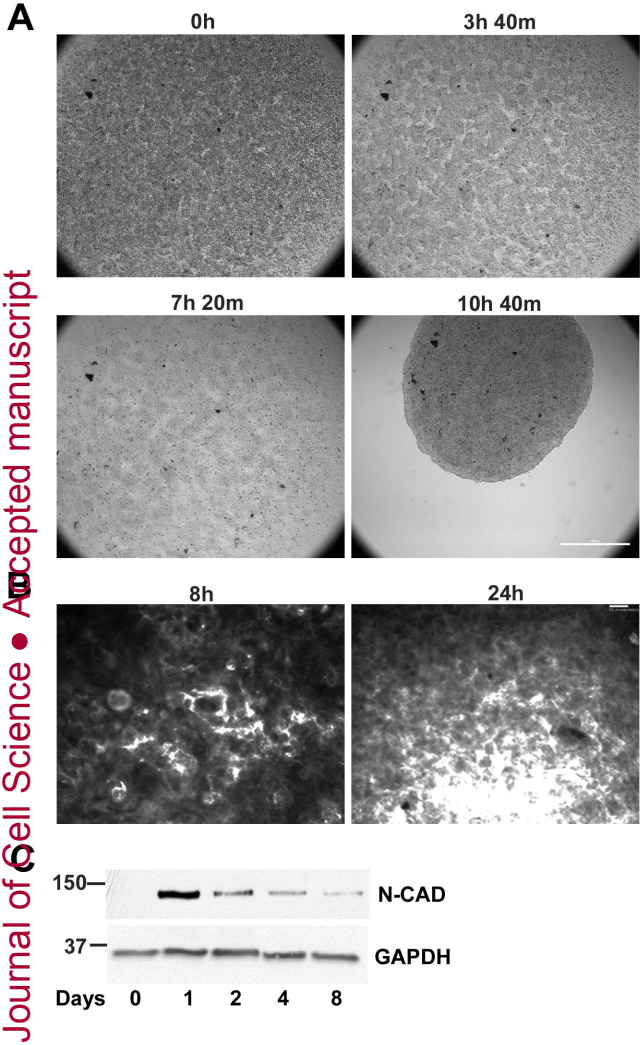

Figure 1

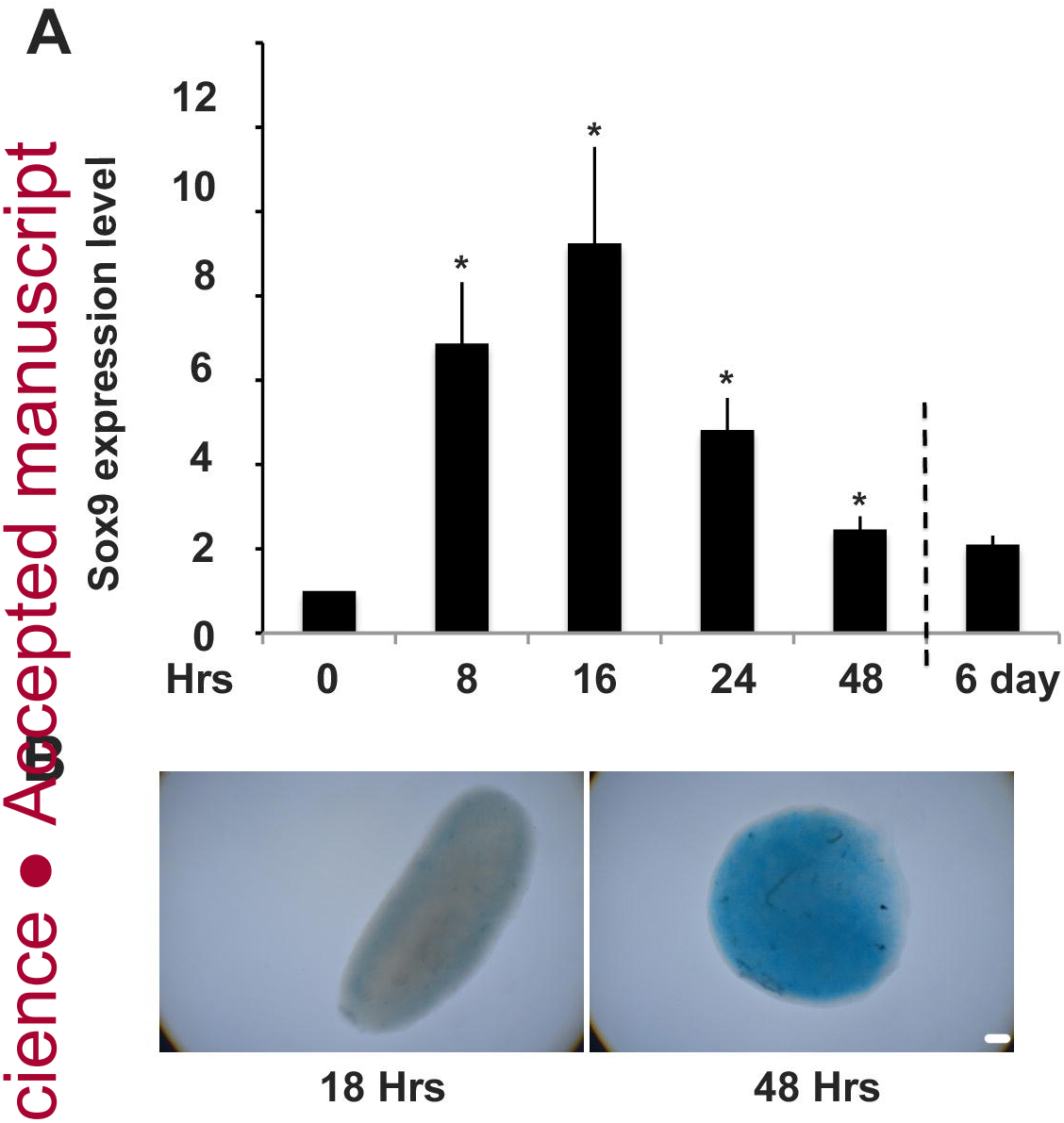

Figure 2

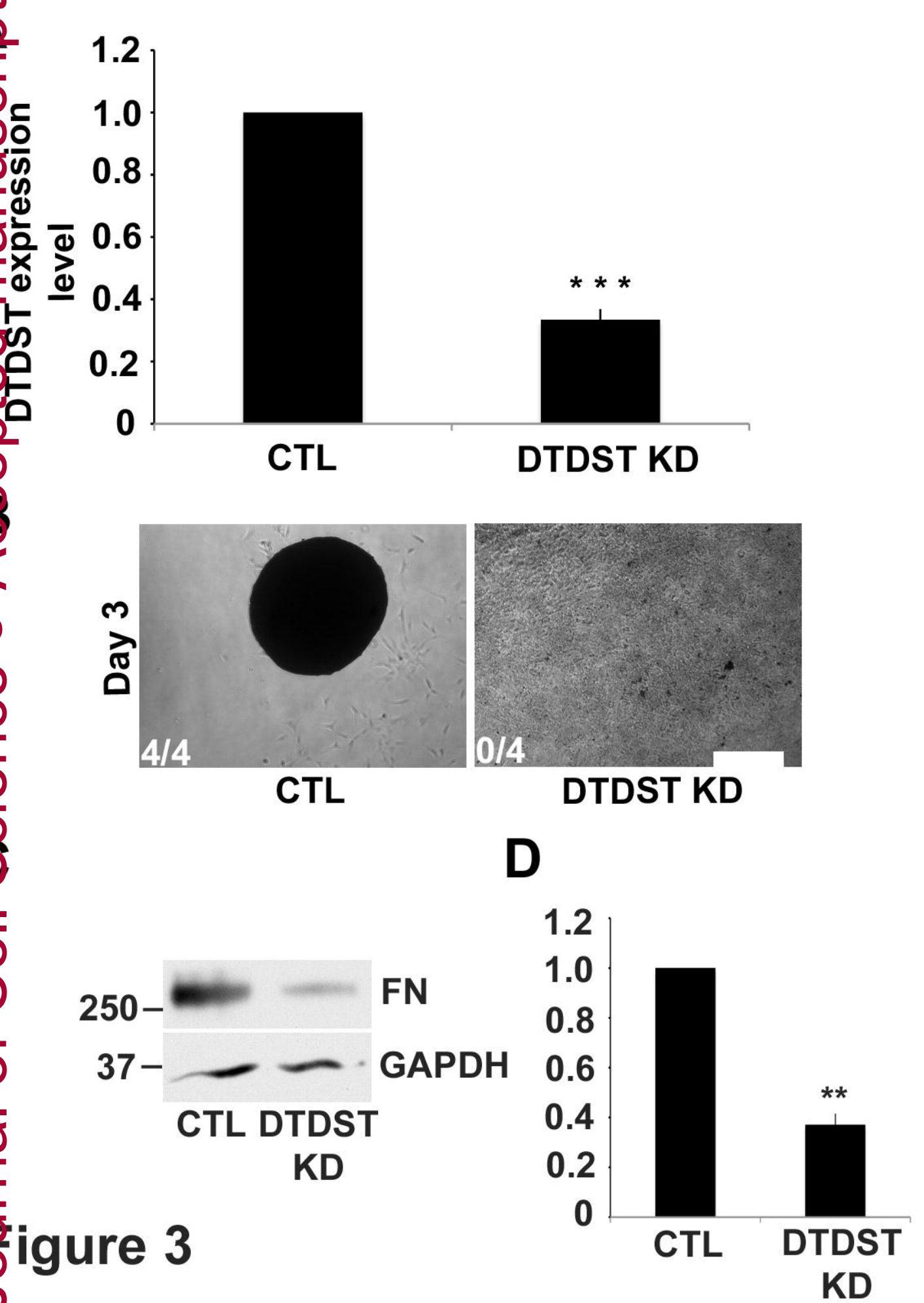

Figure 3

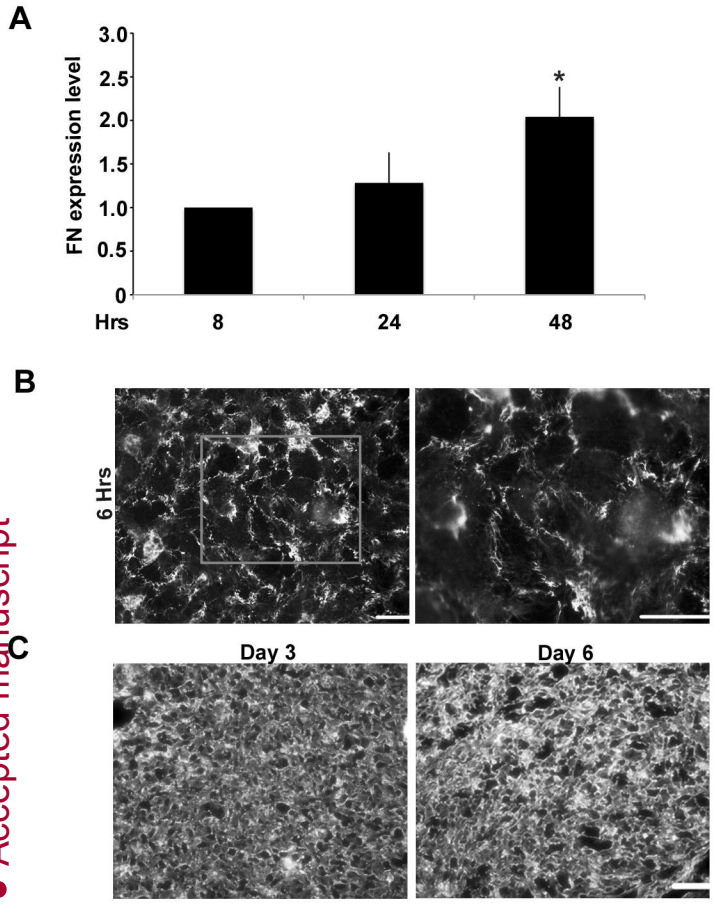

Figure 4

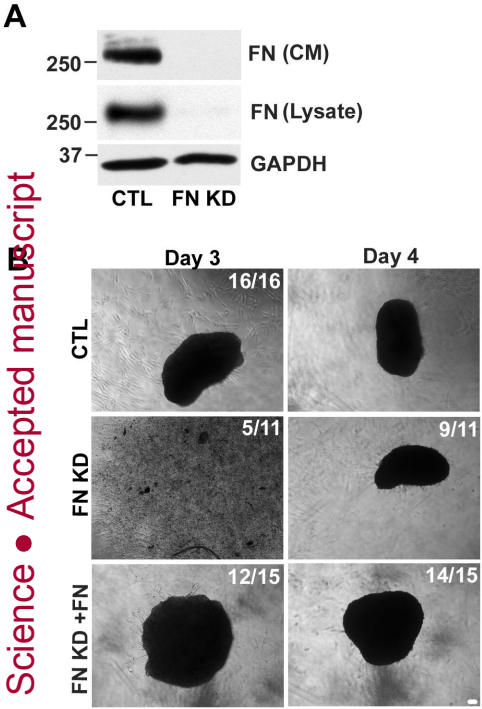

Figure 5

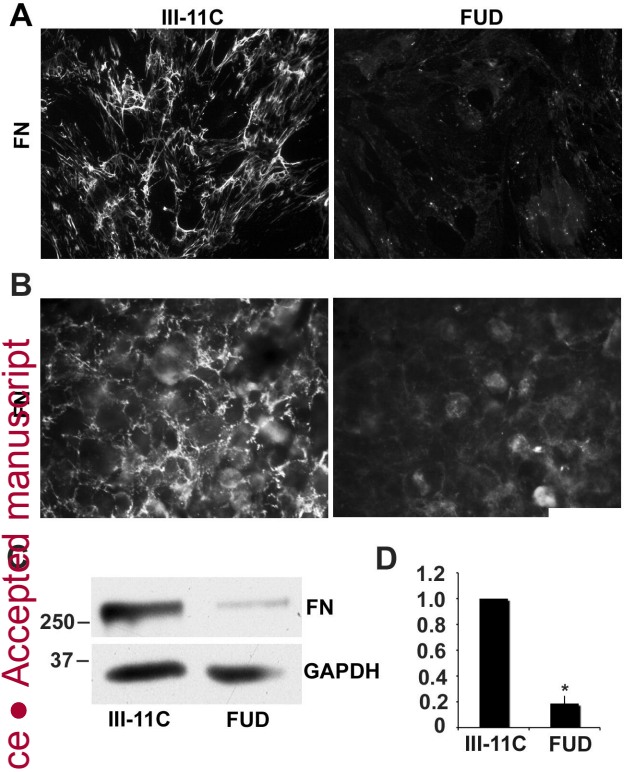

Figure 6

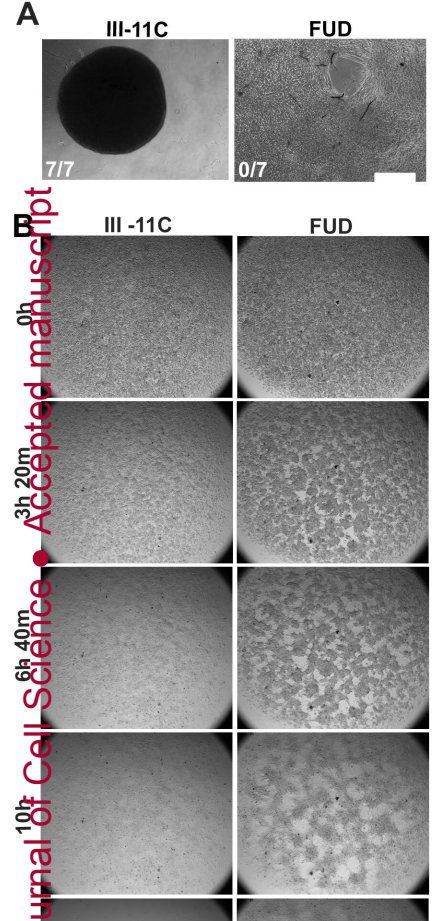

Figure 7

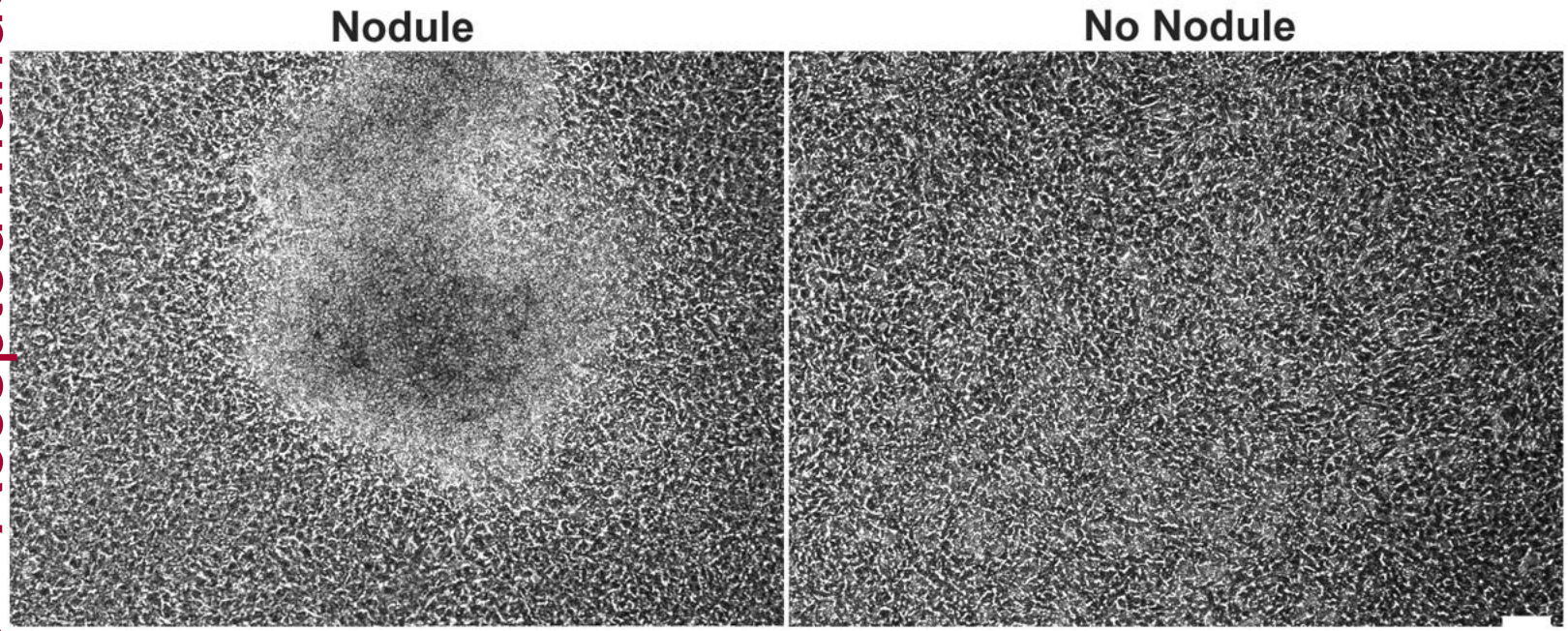

B

Nodule formation

III-11C	FUD
35	6

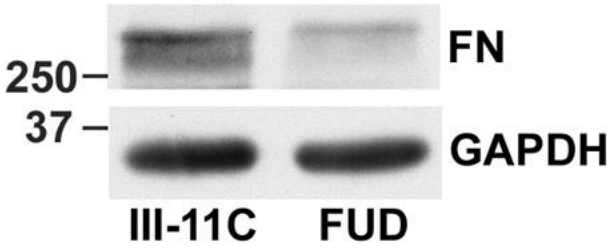

Figure 8